

Aggregatibacter actinomycetemcomitans leukotoxin cytotoxicity occurs through bilayer destabilization

Angela C. Brown,¹ Kathleen Boesze-Battaglia,² Yurong Du,¹ Frank P. Stefano,² Irene R. Kieba,^{1†} Raquel F. Epand,³ Lazaros Kakalis,⁴ Philip L. Yeagle,^{4,5} Richard M. Epand³ and Edward T. Lally^{1*}

Departments of ¹Pathology and ²Biochemistry, University of Pennsylvania School of Dental Medicine, Philadelphia, PA 19104, USA.

³Department of Biochemistry and Biomedical Sciences, McMaster University, Hamilton, Ontario L8S 4 K1, Canada.

⁴Department of Chemistry, Rutgers University, Newark, NJ 07102, USA.

⁵Faculty of Arts and Sciences, Rutgers University, Newark, NJ 07102, USA.

Summary

The Gram-negative bacterium, *Aggregatibacter actinomycetemcomitans*, is a common inhabitant of the human upper aerodigestive tract. The organism produces an RTX (Repeats in ToXin) toxin (LtxA) that kills human white blood cells. LtxA is believed to be a membrane-damaging toxin, but details of the cell surface interaction for this and several other RTX toxins have yet to be elucidated. Initial morphological studies suggested that LtxA was bending the target cell membrane. Because the ability of a membrane to bend is a function of its lipid composition, we assessed the proficiency of LtxA to release of a fluorescent dye from a panel of liposomes composed of various lipids. Liposomes composed of lipids that form nonlamellar phases were susceptible to LtxA-induced damage while liposomes composed of lipids that do not form non-bilayer structures were not. Differential scanning calorimetry demonstrated that the toxin decreased the temperature at which the lipid transitions from a bilayer to

a nonlamellar phase, while ³¹P nuclear magnetic resonance studies showed that the LtxA-induced transition from a bilayer to an inverted hexagonal phase occurs through the formation of an isotropic intermediate phase. These results indicate that LtxA cytotoxicity occurs through a process of membrane destabilization.

Introduction

A secreted leukotoxin (LtxA) plays a key role in the virulence of *Aggregatibacter actinomycetemcomitans* (Zambon, 1985; Tsai and Taichman, 1986). LtxA is a member of the repeats in toxin (RTX) family, which includes an α -haemolysin produced by *Escherichia coli* and the adenylate cyclase toxin (ACT) produced by *Bordetella pertussis*, the causative agent of whooping cough. LtxA shares with the other members of the family a common operon organization and the functional domains of its structural toxin gene product. LtxA is synthesized as an inactive protoxin from the *ltxA* gene, which is part of a four-gene operon (*ltxC*, *ltxA*, *ltxB*, *ltxD*). LtxC is an acyltransferase, which activates the structural toxin gene product (proLtxA) through covalent post-translational acylation at the ϵ -amino groups of Lys⁵⁶² and Lys⁶⁸⁷ (Fong *et al.*, 2011). LtxB and LtxD, along with TdeA (Crosby and Kachlany, 2007), a TolC homologue (Balakrishnan *et al.*, 2001), form a type I secretion system that facilitates the secretion of the toxin directly from the bacterial cytoplasm into the extracellular environment. The structural toxin gene product (LtxA) contains 1055 residues that are organized into four functional domains (Lally *et al.*, 1989), archetypal for the RTX family, consisting of (i) an N-terminal hydrophobic domain composed of α -helices, some of which are amphipathic helices, structures often associated with transmembrane segments or protein pores, (ii) a central region recognized by the acyltransferase, (iii) a repeat region containing 14 canonical nonapeptide repeat units with the sequence [(L/I/F)-X-G-G-X-G-(N/D)-D-X] that forms a calcium-binding site (Baumann and Mueller, 1974; Lally *et al.*, 1991), and (iv) the C-terminal domain, which is required for secretion of the toxin (Jarchau *et al.*, 1994).

Although LtxA is believed to be a membrane-damaging toxin, the mechanistic details of the interaction of the toxin with the lipid bilayer of the cell remain unknown, as

Received 14 October, 2011; revised 28 December, 2011; accepted 13 January, 2012. *For correspondence. E-mail lally@toxin.dental.upenn.edu; Tel. (+215) 898 5913; Fax (+215) 898 2050.

This work was supported by NIH grants R01 DE09517 to E.T.L., F32 DE020950 to A.C.B., R01 EY010420 to K.B.B. and Canadian Institutes of Health Research Grant MOP 86608 to R.M.E.

[†]Deceased.

structural models of LtxA and the other RTX toxins are not currently available. Early studies (Ludwig *et al.*, 1998) suggested that RTX-induced cell death is the result of toxin-generated transmembrane pores that disrupt the ability of the cell to maintain osmotic equilibrium. Evidence for pore formation by these toxins came through artificial planar bilayer experiments with toxins from *E. coli* (Menestrina *et al.*, 1987; Benz *et al.*, 1989), *Actinobacillus pleuropneumoniae* (Lalonde *et al.*, 1989), *B. pertussis* (Benz *et al.*, 1994), *Proteus vulgaris* and *Morganella morganii* (Benz *et al.*, 2005). LtxA-induced channel conductance was shown to be complex, with multiple open states and voltage-dependent gating, suggesting that a molecular reordering at the toxin–membrane interface may be necessary to induce membrane damage (Lear *et al.*, 1995). This notion is consistent with our observation that LtxA did not spontaneously insert into pre-formed planar lipid bilayers (Lear *et al.*, 1995), but channel activity was observed when the bilayer was broken and reformed in the presence of toxin.

Osmotic protectant experiments have been used to predict the size of pores formed by a number of RTX toxins but initially resulted in disagreement on this issue, with predicted pore sizes ranging from 0.6 nm for *B. pertussis* ACT (Ehrmann *et al.*, 1991) to 3 nm for *E. coli* α -haemolysin (Bhakdi *et al.*, 1986). The LtxA-induced pore size was predicted to be 0.9 nm in diameter (Iwase *et al.*, 1990). Additional studies have revealed that the RTX-induced pore size depends on a number of factors, including temperature, time and toxin concentration, and therefore suggests that rather than being a static process, RTX pore formation is a complex, dynamic process (Moayeri and Welch, 1997).

In the current work, we have studied the nature of the lipid–protein interaction to define the interaction of LtxA with membranes in the context of membrane disruption, using confocal microscopy, scanning electron microscopy

(SEM), fluorescence spectroscopy, differential scanning calorimetry (DSC) and ^{31}P nuclear magnetic resonance (^{31}P NMR) to gain an understanding of this initial, yet vital, interaction. Fluorescently labelled toxin was found to associate with immune cell membranes in the form of protein-rich ‘domains’. SEM demonstrated that human immune cell lines incubated with LtxA for 30 min were smoothed and contained large depressions; after 3 h, the toxin-treated cells contained large, lipid-lined cavities, suggesting that LtxA had deformed the cell membrane. We then investigated the membrane-disrupting ability of LtxA as a function of lipid composition and found that LtxA induces significant leakage of a fluorescent dye from liposomes composed of lipids favouring formation of nonlamellar phases but not from liposomes containing lipids that preclude formation of nonlamellar phases. DSC showed that LtxA causes a dose-dependent bilayer disruption while the ^{31}P NMR studies revealed that this transition involves a change from a bilayer to an isotropic intermediate phase, followed by an inverted hexagonal (H_{II}) phase. From our current studies, we conclude that rather than forming a transmembrane pore, LtxA mediates membrane damage by modifying the membrane bilayer structure.

Results

LtxA clusters on immune cell membranes

Fluorescein isothiocyanate (FITC)-labelled LtxA (4×10^{-6} M) was incubated with 1×10^6 Jn.9 cells (Cherry *et al.*, 2001) (30 min, 37°C), stained with wheat germ agglutinin-Alexa Fluor 594 (WGA-AF594), and examined by confocal microscopy to visualize the association of LtxA with the target cell membrane. LtxA was found to be clustered on the target cell surface (Fig. 1), with most cells containing several LtxA-rich clusters. The membrane appeared to be continuous, and no breaks, which would indicate pore formation, were observed.

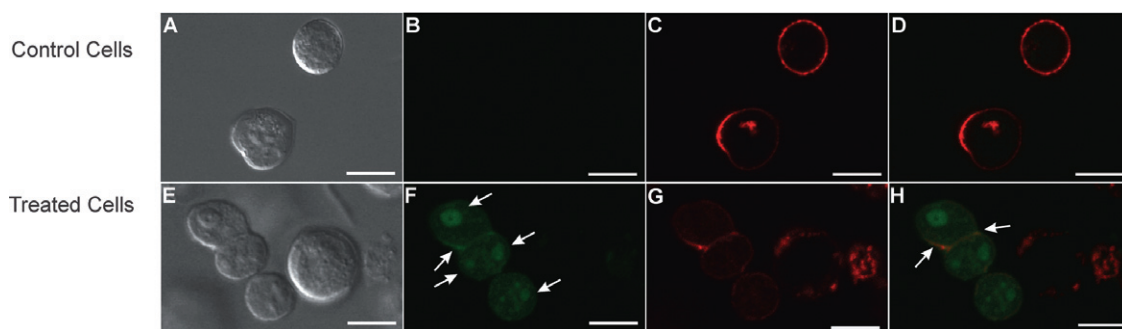


Fig. 1. Localization of fluorescein-labelled LtxA on the surface of target cells. Top row: untreated control cells, Bottom row: LtxA-treated (30 min) cells.

A and E. Phase contrast image.

B and F. FITC (LtxA) stain. Arrows indicate LtxA clusters.

C and G. WGA-AF594 (membrane) stain.

D and H. FITC and WGA-AF-594 merge. Arrows indicate colocalization. Bar = 10 μm .

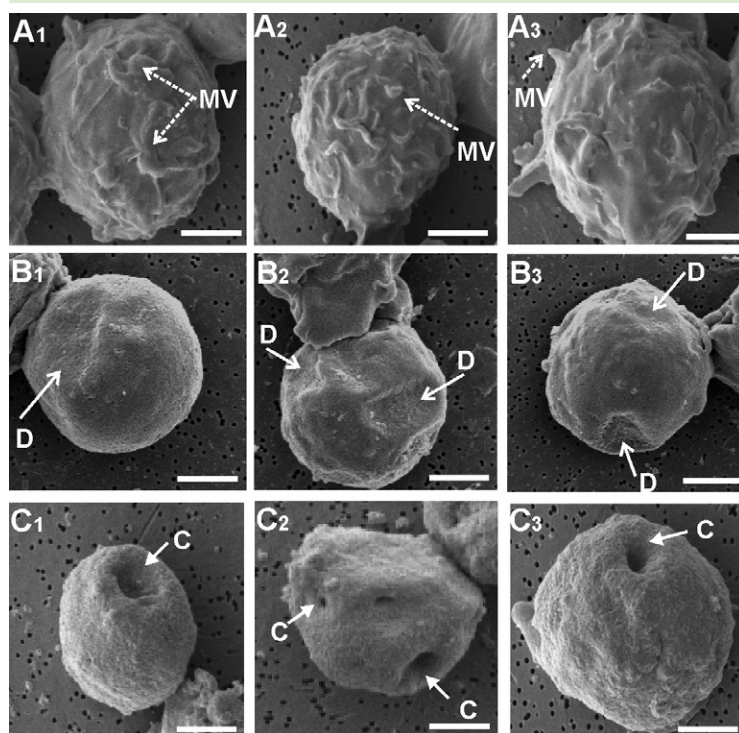


Fig. 2. LtxA mediates collapse of microvilli on Jn.9 target cells. The samples were prepared for conventional scanning electron microscopy of an untreated control (Fig. 2A_{1–3}) and experimental groups after 30 min (Fig. 2B_{1–3}) and 3 h (Fig. 2C_{1–3}) of incubation with LtxA (1×10^{-9} M). Images are representative of the unique phenotypes observed within each group in three independent experiments. All images were acquired at $\times 6000$ and bars equal 2.5 μ m. MV, microvilli; D, depression; C, cavity.

LtxA induces morphological changes in immune cell membranes

Jn.9 cells (5×10^6 cells m^{-1}) were incubated at 37°C with LtxA (10^{-9} M). Cells were removed after 30 min and 3 h, fixed in Karnofsky's solution and examined on a JEOL JSM-T330A scanning electron microscope. The untreated control cell surfaces (Fig. 2A_{1–3}) contained short, stubby projections (microvilli) on the surface. A change in surface membrane morphology, however, was observed in cells exposed to LtxA. We observed a collapse of the microvilli and membrane ruffles, resulting in a smooth cell surface in this group (Fig. 2B_{1–3}). Focal depressions (D) on the membrane surface were also a prominent feature of this experimental group. Three hours following toxin exposure, multiple large cavities (C) were observed to arise from these depressions in most of the target cell membranes (Fig. 2C_{1–3}).

The LtxA-induced membrane lesions were then examined in greater detail using Ga³⁺ focused ion beam (FIB) sections (Fig. 3). Control cells again showed the presence of microvilli on the surface (Fig. 3A₁), and the FIB cut-cell surface was contiguous (Fig. 3A₂). The membrane depressions we observed after a 30 min toxin treatment could also be seen on the cut section but did not demonstrate gross evidence of membrane damage (Fig. 3B_{1–3}). Closer examination of the concavities (Fig. 3C_{1–3}) revealed that the outer and inner surfaces of the cell membrane could be visualized throughout the course of these depressions and suggests that the origin

may be a toxin-induced bending of the structure. An irregular tear in the membrane could be seen at the base of the defect (Fig. 2C₄), further suggests that the mechanism of membrane disruption weakens the membrane.

LtxA-induced morphological changes are lipid-dependent

The distinct toxin-induced changes in immune cell morphology suggest that LtxA may disrupt the stable bilayer structure of the cell membrane. Because lipid composition and the subsequent phase behaviour determine membrane structure, we investigated the membrane-disrupting ability of LtxA as a function of lipid composition, specifically in terms of the types of structures adopted by each lipid. Saturated phosphatidylcholines (PCs), such as 1,2-dipalmitoyl-*sn*-glycero-3-phosphocholine (DPPC), form flat, bilayer structures (Fig. 4A, top panel), and saturated lysoPCs, such as 1-stearoyl-2-hydroxy-*sn*-glycero-3-phosphocholine (SPC), form micelles or hexagonal (H_I) phases (Fig. 4A, centre panel). Phosphatidylethanolamines (PEs), such as 1,2-dimyristoyl-*sn*-glycero-3-phosphoethanolamine (DMPE), which have a more hydrophobic headgroup than PC (Yeagle and Sen, 1986), form nonlamellar structures including cubic and inverted hexagonal (H_{II}) phases (Fig. 4A, bottom panel) to minimize contact of the headgroup with water (Yeagle and Sen, 1986).

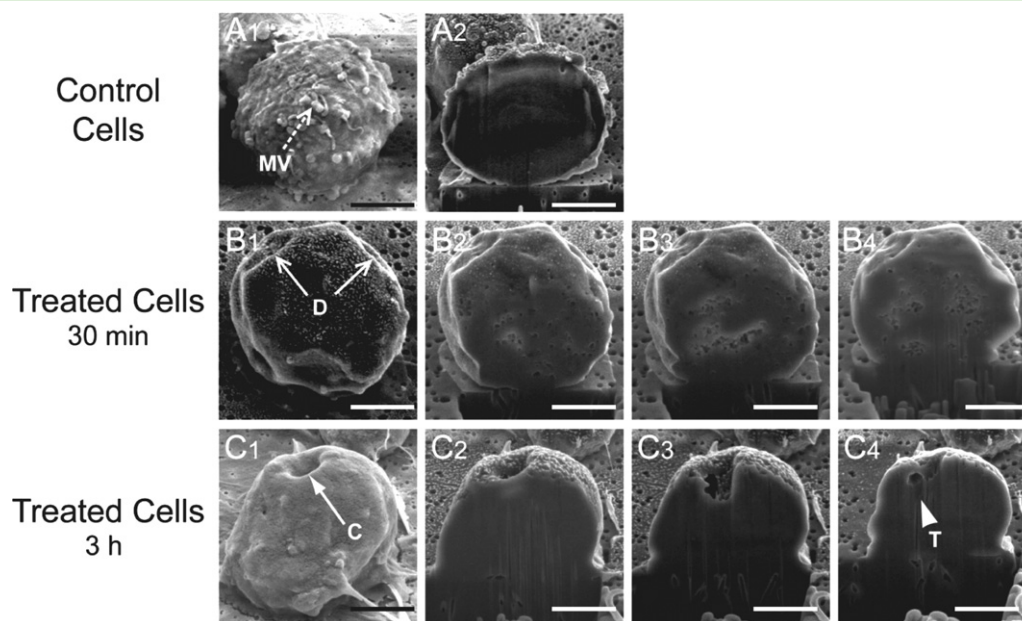


Fig. 3. SEM images of LtxA-treated Jn.9 cells.

A. Jn.9 cell, which has not been exposed to LtxA. This control cell was sliced coronally with a Ga^{3+} FIB (A₁).

B. Jn.9 cell exposed to LtxA (1×10^{-9} M) for 30 min.

C. Jn.9 cell exposed to LtxA (1×10^{-9} M) for 3 h. The toxin-treated cells were serially sliced coronally with the FIB (B₂–B₄ and C₂–C₄). MV, microvilli; D, depression; C, cavity; T, tear. Bar = 5 µm.

To identify the mechanism of membrane disruption by LtxA, we studied LtxA-induced leakage from fluorescent dye (calcein)-encapsulating liposomes. The liposomes contained the di-saturated PC, DPPC, in one of three compositions: (i) 100% DPPC, (ii) DPPC and SPC (3:1), or (iii) DPPC and DMPE (3:1). The leakage experiments were performed at a temperature of 30°C. LtxA-induced membrane disruption was measured by release of the dye from liposomes treated with toxin in a dose-dependent manner.

Representative leakage profiles from liposomes composed of each of these lipid combinations, treated with toxin (mole fraction of 0.0013), are shown in Fig. 4B. The extent of leakage after 30 min of LtxA exposure is shown in Fig. 4C for all three lipid compositions, at six toxin concentrations. As shown in Fig. 4C, calcein leakage from toxin-treated liposomes containing only DPPC was very low at all toxin levels, but increased slightly with increasing mole fractions of LtxA. Similarly, almost no calcein leaked from toxin-treated liposomes composed of DPPC/SPC (3:1); however, in contrast to DPPC liposomes, in these liposomes, an increase in LtxA mole fractions did not increase leakage. Compared with these two liposome types, leakage from toxin-treated liposomes composed of DPPC/DMPE (3:1) was significant and dose-dependent. These results suggest that membrane disruption is most favourable in toxin-treated liposomes containing some DMPE and is

entirely unfavourable in toxin-treated liposomes containing SPC.

Because LtxA-mediated membrane disruption is greatly enhanced by the presence of DMPE and inhibited by the presence of SPC, the results suggest that formation of a H_{II} phase may play a role in the toxin's mode of action. We therefore investigated the effect of two lipids that inhibit H_{II} phase formation, SPC (Fuller and Rand, 2001) and the bilayer stabilizer, cholesterol sulfate (CS) (Cheetham *et al.*, 1990), on LtxA-induced membrane disruption in liposomes containing DMPE. Leakage was measured from liposomes composed of either DPPC/DMPE/SPC (2:1:1) or DPPC/DMPE/CS (2:1:1) and treated with toxin (mole fraction of 0.001). Leakage from LtxA-treated liposomes composed of DPPC/DMPE/SPC (2:1:1) was substantially reduced relative to the leakage from toxin-treated liposomes composed of DPPC/DMPE (3:1) (Fig. 4D), indicating that SPC inhibits LtxA membrane disruption in these PE-containing liposomes. In addition, leakage from toxin-treated liposomes composed of DPPC/DMPE/CS (2:1:1) was reduced to an even greater extent (Fig. 4D) at the same toxin mole fraction. These results demonstrate that the membrane disruption that is favoured in PE-containing membranes is inhibited by lipids that inhibit nonlamellar phase formation, suggesting that LtxA membrane disruption might proceed through the formation of a nonlamellar lipid phase (Fuller and Rand, 2001; Epand, 2007).

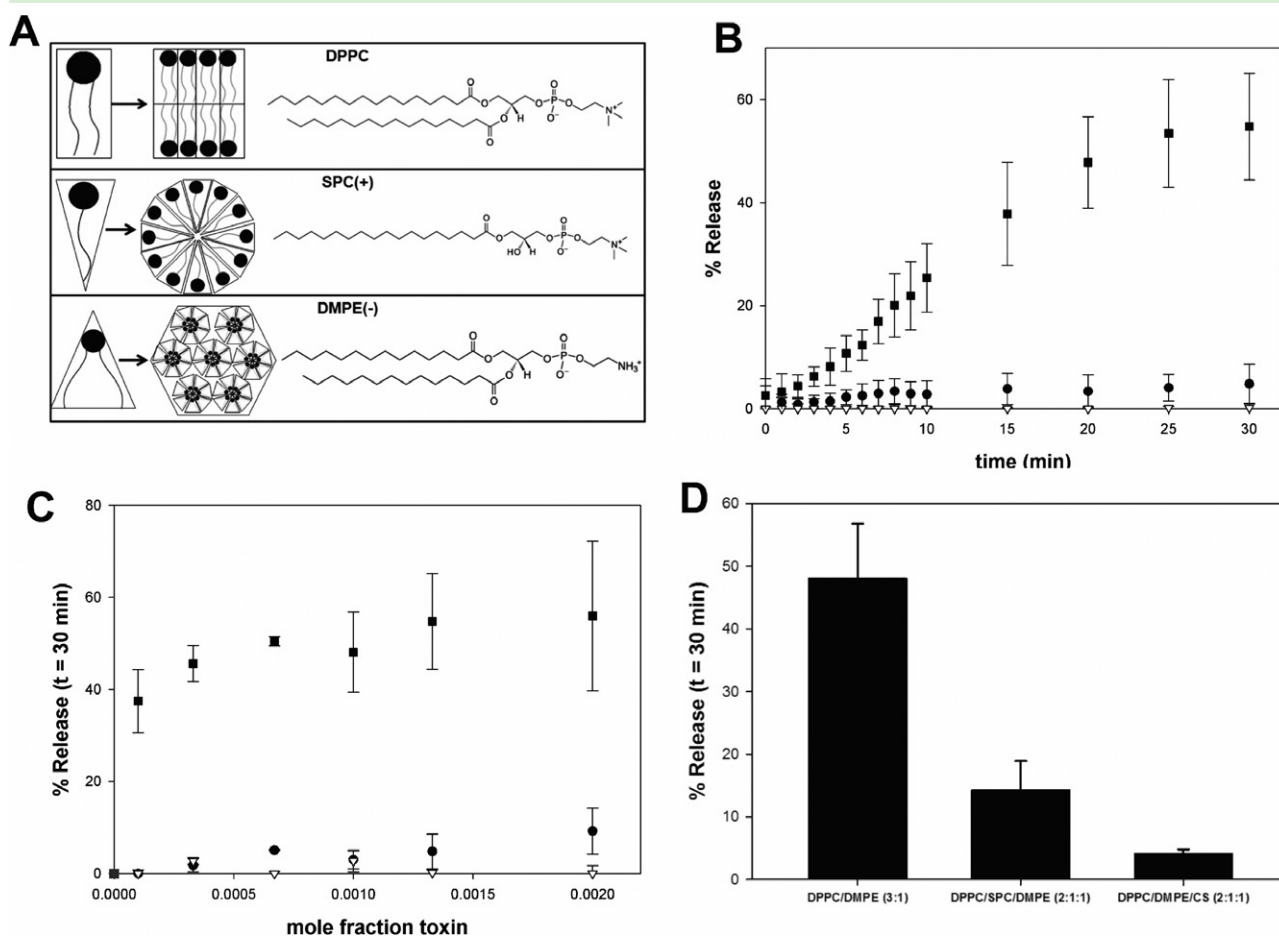


Fig. 4. LtxA-induced leakage of calcein.

A. Structure of the lipids used in the leakage study.

B. Representative scans of leakage at a protein mole fraction of 0.0013 from liposomes composed of DPPC (100%) (●), DPPC/SPC (3:1) (▽) and DPPC/DMPE (3:1) (■).

C. Leakage of calcein after 30 min of incubation with LtxA for liposomes composed of DPPC (100%) (●), DPPC/SPC (3:1) (▽) and DPPC/DMPE (3:1) (■).

D. LtxA-induced leakage of calcein at a protein mole fraction of 0.0010 for liposomes composed of DPPC (100%), DPPC/SPC (3:1), DPPC/DMPE (3:1), DPPC/DMPE/SPC (2:1:1) or DPPC/DMPE/CS (2:1:1). Results are statistically significant ($P < 0.001$) for differences between the control (DPPC/DMPE) and both DPPC/DMPE/SPC and DPPC/DMPE/CS.

LtxA destabilizes membrane structure by inducing a lipid phase change

To determine if LtxA induces a lipid phase change (from a bilayer to H_{II} phase) in the membrane of the target cells, both DSC and ^{31}P NMR were employed. The DSC experiments examined a shift in the bilayer-to- H_{II} (nonlamellar) phase transition temperature (T_H) of 1,2-dipalmitoleoyl-*sn*-glycero-3-phosphoethanolamine (di16:1-PE). This lipid was chosen because it has a T_H of 44.5°C and therefore avoids the need for scanning at higher temperatures at which the toxin may become denatured. The effect of the progressive addition of LtxA to di16:1-PE liposomes was measured to determine the toxin's effect on the transition of the lipid from a lamellar (bilayer) to a H_{II} phase (Fig. 5A). The peak in each DSC scan represents the T_H ,

with the membrane existing in a bilayer phase at temperatures below the T_H and in an H_{II} phase at temperatures above the T_H .

In the absence of LtxA, the T_H of di16:1-PE is 44.5°C; addition of toxin resulted in peak broadening and a shift of the T_H to lower temperatures. Regression analysis of the curve of T_H as a function of the mol fraction of toxin resulted in a slope of -7570 ± 1400 (Fig. 5B). The sensitivity of the T_H to LtxA and the direction of the shift to lower temperatures provide a strong indication that the toxin is a potent modulator of membrane structure and acts by disrupting the bilayer through the formation of a nonlamellar phase.

The nature of this toxin-induced non-bilayer phase was studied using ^{31}P NMR. The ^{31}P NMR spectra of multilamellar liposomes composed of 1,2-dioleoyl-*sn*-glycero-3-

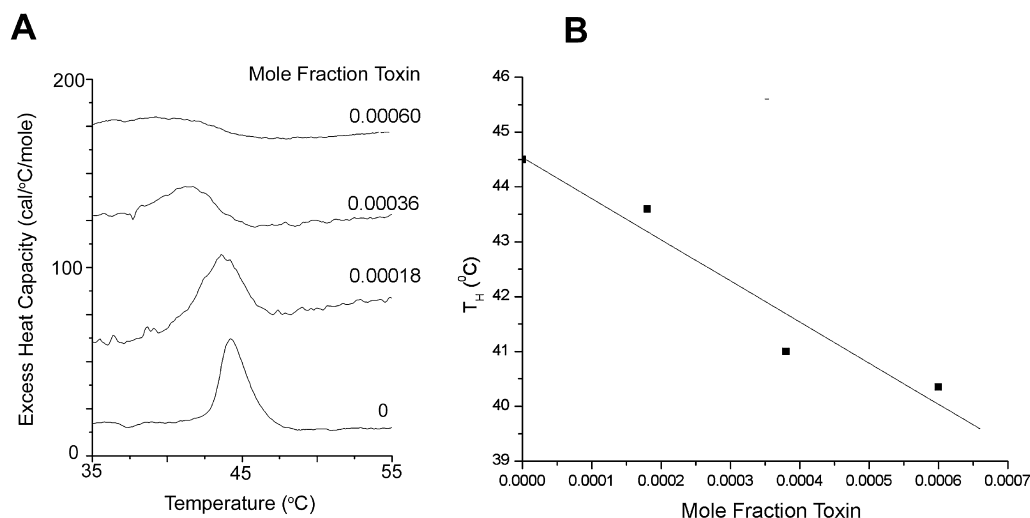


Fig. 5. Effect of LtxA on bilayer-to-hexagonal phase transition of di16:1 PE.

A. Raw DSC scans showing the phase transition temperature of liposomes treated with increasing concentrations of LtxA. B. T_H of each scan as a function of LtxA mol fraction.

phosphoethanolamine-N-methyl (N-methyl DOPE) were collected as a function of temperature, either without toxin (–LtxA) or with a toxin mole fraction of 0.0001 (+LtxA). This particular lipid was chosen because of its well-studied phase behaviour (Boesze-Battaglia *et al.*, 1992; van Gorkom *et al.*, 1992; Siegel and Tenchov, 2008) and its experimentally convenient T_H of 55°C, which prevents the need for extreme temperature scans.

Without toxin treatment, the liposomes composed of N-methyl DOPE were found to exist in a bilayer phase at temperatures between 10°C and 40°C, as evidenced by the maximum in the spectra at a chemical shift of approximately –14 p.p.m. and from the shape of the powder pattern (Fig. 6A). At 50°C, both bilayer (–14 p.p.m.) and isotropic peaks (maximum at 0 p.p.m.) were observed, indicating that at this temperature, the lipid was in the transition between the bilayer and a nonlamellar phase. At temperatures of 60°C and above, an isotropic (0 p.p.m.) peak was observed, along with a maximum at a chemical shift of approximately 6 p.p.m., corresponding to the H_{II} phase (Fig. 6A). Treatment of these liposomes with a toxin mole fraction of 0.0001 altered this behaviour significantly (Fig. 6B). At a temperature of 10°C, both bilayer (–14 p.p.m.) and isotropic (0 p.p.m.) peaks were observed in toxin-treated liposomes, and the relative intensity of these maxima shifted with increasing temperatures, indicating a temperature-dependent increase in the isotropic nature and a decrease in the bilayer nature of the membrane. At 50°C, the H_{II} (6 p.p.m.) and isotropic (0 p.p.m.) peaks dominated, but a small bilayer (–14 p.p.m.) peak remained. As the temperature increased to 60°C and 70°C, the bilayer (–14 p.p.m.) peak disappeared, leaving only the H_{II} (6 p.p.m.) and isotropic (0 p.p.m.) peaks.

Discussion

The interaction of LtxA with the membrane of a susceptible cell disrupts the selective barrier function performed by this structure. The process is complex, especially when one attempts to generate unifying hypotheses from observations obtained from experiments with individual RTX toxins. The current report has focused on LtxA to characterize the modifications induced by this toxin to the bilayer structure of both cells and model membranes. In our studies, the use of model membranes demonstrated the ability of LtxA to perturb a stable planar bilayer arrangement. Although it is possible to construct liposomes that contain the same lipids as the plasma membranes of immune cells, the systems would still be expected to behave quite differently because there would be no proteins or transmembrane asymmetry in the model membrane system. Furthermore, one cannot measure isotropic peaks in liposomes with these ‘natural’ lipid mixtures. Therefore, the liposomes utilized in our studies were not meant to be models for the biological membrane but rather as sensitive indicators of protein-induced bilayer perturbation.

We demonstrated that LtxA associates with the immune cell membrane in clustered, LtxA-rich regions (Fig. 1). The morphological changes caused by the association of LtxA with the membrane were investigated using SEM (Fig. 2). These studies clearly demonstrated two types of toxin-induced membrane defects: (i) collapse of the microvilli normally present on the outer surface of the cells and (ii) the formation of cell surface depressions and then cavities. Hemi-sectioning of individual cells through these membrane defects with a Ga^{3+} beam showed that the

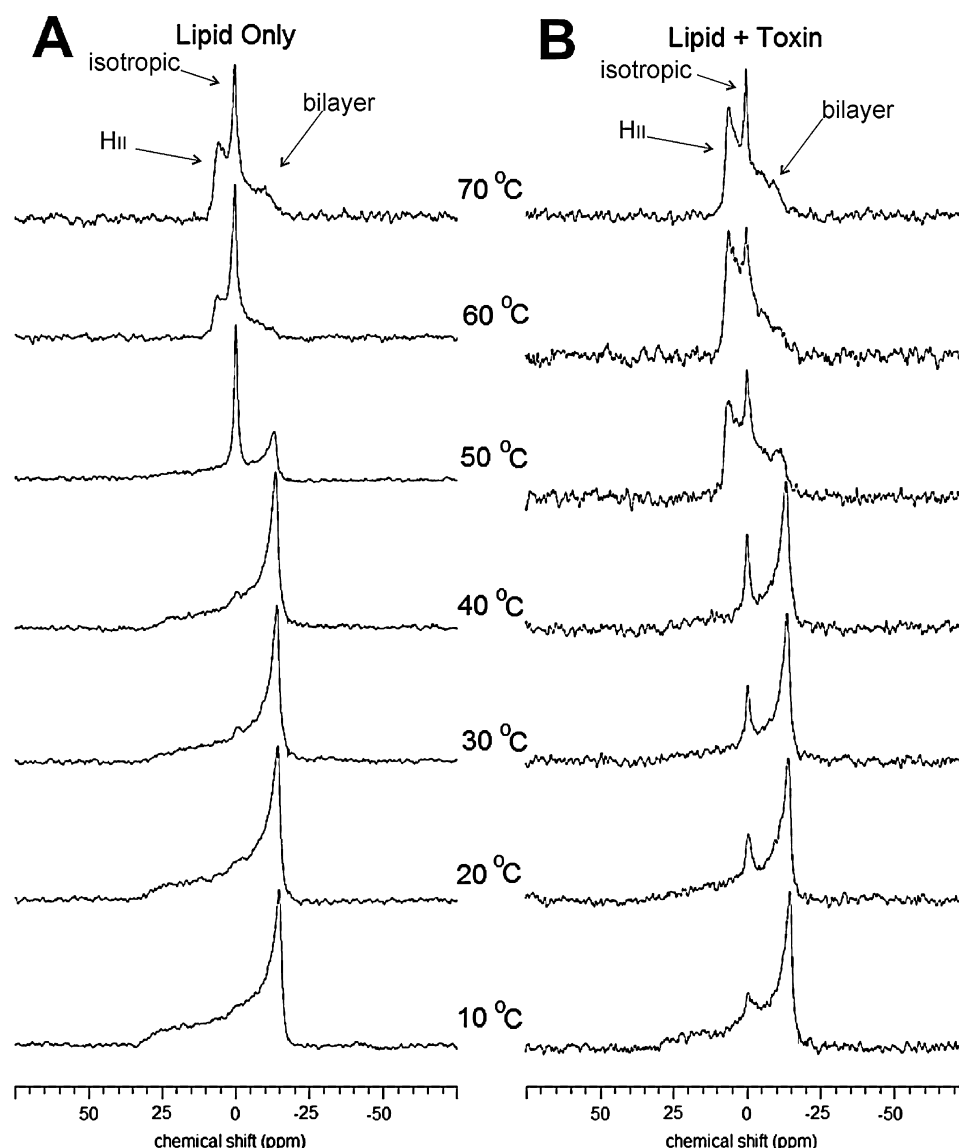


Fig. 6. ^{31}P NMR spectra of N-methyl-DOPE liposomes.

A. N-methyl-DOPE liposomes without LtxA.

B. N-methyl-DOPE liposomes treated with an LtxA mole fraction of 0.0001. Spectra were collected at 10°C, 20°C, 30°C, 40°C, 50°C, 60°C and 70°C.

surface of the cavity retained a similar morphology as the surface of the cell, suggesting that the cavities are lipid-lined. In addition, the membrane appears to be continuous through the cross-section of the depression, thereby suggesting that the disruptions are being produced by a toxin-induced weakening of the membrane.

The results presented here likely exclude the possibility of LtxA forming a barrel-stave pore, in which the protein inserts directly into a membrane to form a protein-lined annulus (Baumann and Mueller, 1974; Sansom, 1991). Toroidal pore formation was likewise excluded by the effect of lipid composition on LtxA-induced pore formation in calcein-loaded liposomes composed of combinations of

lipids (Fig. 3). Melittin, a known toroidal pore former, has been shown to induce leakage to a greater extent from liposomes containing lyso-lipids and to a lesser extent from liposomes containing PEs and other nonlamellar lipids (Allende *et al.*, 2005; Lee *et al.*, 2005). We found that the behaviour of LtxA was exactly opposite; LtxA-induced membrane disruption was significant only in liposomes containing nonlamellar lipids and was significantly less in the membranes composed of bilayer-forming DPPC and/or micelle-forming SPC. Furthermore, LtxA-induced membrane disruption occurred more slowly and to a lesser extent than does melittin-induced leakage (Benachir and Lafleur, 1995; Allende *et al.*, 2005). These

results suggest that toxin-induced membrane disruption does not occur through the formation of a transmembrane pore but may instead be the result of membrane destabilization. The specificity of the interaction of LtxA with membranes containing PEs, which promote the formation of nonlamellar phases, indicated that this destabilization may be related to nonlamellar phase formation. The ability of the nonlamellar phase inhibitors (SPC and CS) to greatly inhibit leakage from PE-containing liposomes (Fig. 4D), further strengthens this argument.

Differential scanning calorimetry and ^{31}P NMR (Figs 5 and 6) were employed to determine if LtxA induces the formation of a nonlamellar phase, and if so, to identify the specific nonlamellar structure that is formed. The DSC studies demonstrated that LtxA is a potent nonlamellar phase inducer whose effect on membranes, on a molar basis, rivals classic T_{H} -lowering compounds such as alkanes and diacylglycerols (DAGs) (Erand, 2002). The ^{31}P NMR experiment further revealed that the LtxA-induced nonlamellar phase induction occurs by promotion of the H_{II} phase through an isotropic intermediate. In addition, both DSC and ^{31}P NMR demonstrated that LtxA broadens the transition temperature from the bilayer to the nonlamellar phases. Along with lowering T_{H} and broadening the transition, the toxin increased the relative amount of H_{II} phase that was formed at temperatures above T_{H} . For example, at 60°C , in the absence of toxin, the membrane primarily consisted of an isotropic phase, with a small amount of H_{II} phase, as evidenced by the relative peak intensities at approximately 0 p.p.m. and 6 p.p.m. respectively. At this same temperature, in the presence of toxin, the isotropic and H_{II} peaks were approximately equal in height, indicating that the toxin increased the relative amount of H_{II} phase.

The dimensions of the structure giving rise to the isotropic ^{31}P NMR spectra could range from less than 100 nm (micelle) to several microns (cubic phase structure). Furthermore, it is not possible to compare the measurements of the structures represented by the NMR spectra with the features observed in the cell membrane by SEM except to say that both are the result of destabilization of the lipid bilayer structure of the membrane by LtxA. Previously, we have shown that LtxA binding to LFA-1 induces the formation of large LtxA-LFA-1 and cholesterol-rich rafts. The cell surface depressions observed on the SEM micrographs may be a consequence of LFA-1- and cholesterol-dependent clustering; however, the fact that it is sunken suggests that the bilayer disruption plays a role in this process as well.

Smoothing of the cell membrane caused by the collapse of microvilli is a feature of T cells that occurs as a result of integrin activation and cleavage from the cytoskeleton (Burkhardt *et al.*, 2008). Certain aspects of the interaction between LtxA and LFA-1 have been shown to

mimic 'outside-in' integrin activation signals such as elevation of cytosolic Ca^{2+} , activation of calpain, talin cleavage and clustering of LFA-1 and LtxA in the raft compartment (Fong *et al.*, 2006).

Previous work in our lab and others' has shown that LFA-1 is required for cytotoxicity of LtxA (Lally *et al.*, 1997; Dileepan *et al.*, 2007; Kieba *et al.*, 2007); however, the current report has shown that membrane disruption is occurring in liposomal systems that do not contain LFA-1. The reasons for this observation are not clear, although it has been shown that LtxA will lyse sheep red blood cells under certain conditions (Balashova *et al.*, 2006). In previous work, we produced, screened, and mapped the epitopes of a panel of monoclonal antibodies that inhibited LtxA killing of HL-60 cells (Lally *et al.*, 1994). The inhibitory antibodies segregated in one of three epitopes: (i) epitope A, composed of residues 698–709, which are near one of two LtxA acylation sites (Lys687) (Fong *et al.*, 2011), (ii) epitope B (residues 746–757), containing the second and third glycine-rich repeats, and (iii) epitope C (residues 926–937), a region that is distal to the glycine repeats. The identification of three 'inhibitory' epitopes stimulated us to see if the same regions are critical for haemolysis. Monoclonal antibodies to epitope A inhibited toxin-induced red blood cell lysis, while blocking either epitope B or C with an mAb had no effect on haemolysis (Lally *et al.*, 1999). These results suggest that at least two separate processes occur in LtxA killing—membrane disruption leading to haemolysis/osmolysis (associated with epitope A) and a white blood cell-specific interaction (associated with epitopes B and C). This has led us to postulate that LFA-1 binding and bilayer disruption are two separate stages in LtxA-mediated cell death. The interaction of LtxA with liposomes most closely resembles what occurs at epitope A, a non-LFA-1-dependent interaction of LtxA with the membrane that initiates a destabilization of the bilayer. Following this initial membrane contact, engagement of epitopes B and C may well stimulate the apoptotic signal observed by Kelk (Kelk *et al.*, 2003; 2011) through LFA-1 contact.

The presence of nonlamellar lipids in the cell membrane is thought to provide the membrane with structural 'plasticity,' for situations in which a break in the membrane is required, such as fusion or endocytosis (Gruner, 2005). The vital role of nonlamellar lipids in these processes, particularly membrane fusion, has been well studied (Siegel, 2005). In particular, isotropic ^{31}P NMR resonances have been correlated with liposome fusion, indicating that these structures may represent intermediates in the fusion process (Ellens *et al.*, 1989). In addition, divalent cations, particularly Ca^{2+} , have been shown to promote liposome fusion, and in some lipid systems, this is correlated with the ability of cations to promote nonlamellar phases (Ortiz *et al.*, 1992; 1999). It is possible

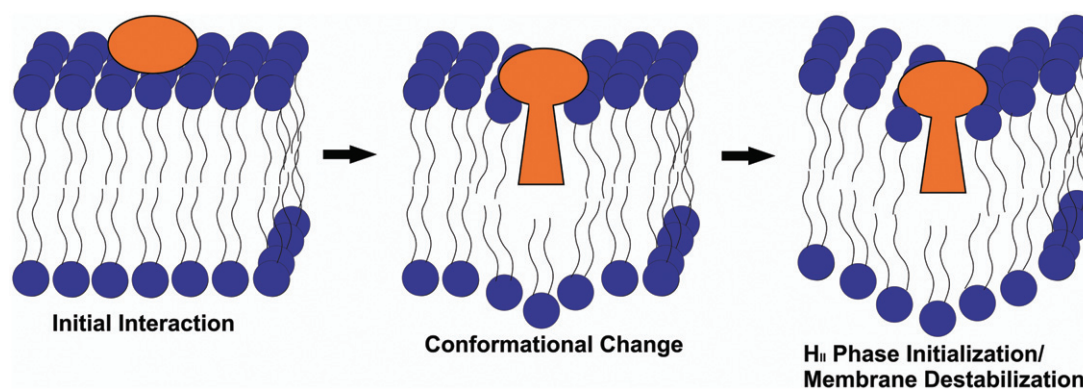


Fig. 7. Proposed model of H_{II}-phase membrane disruption. In this model, the acyl group of LtxA initially contacts the cell membrane, and the toxin undergoes a conformational change in which part of the toxin inserts into the membrane. This induces formation of an isotropic phase, resulting in a destabilization of the membrane.

that the elevation of cytosolic Ca²⁺ that occurs upon initial interaction of the toxin with Jn.9 cells (Fong *et al.*, 2006) may enhance membrane disruption by the toxin, through the promotion of nonlamellar phase formation. Nonlamellar phases have also been proposed to be involved in lipid translocation (Cullis and de Kruijff, 1979), and the induction of these structures by LtxA may be a means by which the toxin penetrates the bilayer. In either case, we propose that LtxA, in its initial interaction with the host cell, takes advantage of the presence of nonlamellar lipids in the membrane, using them to increase the negative curvature strain, thereby destabilizing the membrane bilayer.

The ability to disrupt liposomes containing nonlamellar lipids is a common observation among the various RTX toxins. For example, the *B. pertussis* ACT induces leakage preferentially from liposomes containing PE (Martin *et al.*, 2004), the *Vibrio cholerae* cytotoxin (VCC) induces significant leakage from liposomes containing DAG or ceramide (Zitzer *et al.*, 2001), and the *E. coli* α -haemolysin causes an increase in conductance across bilayers containing PE (Bakas *et al.*, 2006). Interestingly, the nonlamellar lipid dependence of several RTX toxins was hinted at in the early planar bilayer experiments, in which it was widely reported that 'channel' formation by a number of these toxins was significantly more favourable in membranes made of asolectin or PC : PE (5:1) than in pure PC membranes (Menestrina *et al.*, 1987; Benz *et al.*, 1989; 1994; 2005; Maier *et al.*, 1996). Initially, the observation that channel formation is more favourable in asolectin membranes was attributed to either the required presence of multiple lipid components or the possible presence of a receptor in the asolectin membranes. However, because the PC/PE mixture that makes up the major portion of asolectin (McCormick and Johnstone, 1998) is able to adopt a non-bilayer structure, the present data support the possibility that induction of a nonlamellar phase represents a mechanism of membrane disruption

that is conserved among the various RTX toxins. The ability of other protein toxins, such as aerolysin, produced by *Aeromonas hydrophila* (Alonso *et al.*, 2000); sticholysins I and II, produced by *Stichodactyla helianthus* (Valcarcel *et al.*, 2001); equinatoxin II, produced by sea anemones (Anderluh *et al.*, 2003); and streptolysin O (Zitzer *et al.*, 2001), to interact with nonlamellar lipids in model membranes further raises the possibility of nonlamellar phase induction by other protein toxins as well.

We have developed a model, based on the results presented here, to describe the mode of action of LtxA and perhaps other RTX toxins (Fig. 7). In this model, we propose that the hypothesized conformational change in the toxin upon association with the lipid bilayer may allow the hydrophobic residue-rich portion of the toxin to insert into the membrane. This hypothesized conformational change may initiate the formation of nonlamellar structures, thereby weakening the membrane. At this time, it is unknown if the toxin remains associated with the membrane or if it is translocated to the interior of the cell where it may induce further damage. We are currently investigating possible cytoplasmic functions of the translocated toxin, as well as conformational changes in the toxin upon membrane interaction. This model highlights the importance of membrane composition in LtxA-induced membrane disruption, and demonstrates that bilayer disruption is an important initial step in the cytotoxicity of LtxA.

Experimental procedures

Chemicals

Sodium chloride (NaCl), calcium chloride (CaCl₂), sodium azide (NaN₃), 4-(2-hydroxyethyl)piperazine-1-ethanesulfonic acid (HEPES), ethylenediaminetetraacetic acid (EDTA), Trizma base, Sephadex G-50, and calcein were purchased from Sigma Chemical (St Louis, MO, USA). Triton X-100 and potassium phosphate monobasic were purchased from Fisher Scientific.

Lipids, including di16:1-PE, DPPC, DMPE, N-methyl DOPE, and SPC, were purchased from Avanti Polar Lipids (Alabaster, AL, USA). All chemicals were used without further purification.

Cell culture

Jn.9, a subclone of the Jurkat cell line (Cherry *et al.*, 2001) was a gift from Dr. Lloyd Klickstein (Novartis Institute for Biomedical Research, Cambridge, MA, USA). The cells were maintained at 37°C under 5% CO₂ in RPMI 1640 (Mediatech Cellgro, Herndon, VA, USA) containing 10% fetal calf serum (FCS), 0.1 mM MEM non-essential amino acids, 1 × MEM vitamin solution, 2 mM L-glutamine, and 50 µg ml⁻¹ gentamicin.

LtxA purification

Aggregatibacter actinomycetemcomitans, strain JP2, was grown overnight in AAGM broth (Fine *et al.*, 1999). LtxA was purified by precipitating the bacterial culture supernatant with ammonium sulfate (32.5%, 4°C, 2 h) (Kachlany *et al.*, 2002). The precipitate was recovered by centrifugation (10 000 r.p.m., 20 min), suspended in phosphate buffer (10 mM PO₄, pH 6.5), and dialysed overnight. After dialysis, the supernatant was filtered and diluted to 200 ml in phosphate buffer before being applied to a HiTRAP SP column (GE Healthcare, Piscataway, NJ, USA) that had been equilibrated in the same buffer. The column was then washed with phosphate buffer until the optical density (OD₂₈₀) returned to background levels. Next, the buffer was changed to 20% NaCl in phosphate buffer and the column was washed until the protein level again reached background level. Finally, LtxA was eluted with a buffer containing 60% NaCl in phosphate buffer. The toxin was lyophilized and stored at -80°C. The purity of LtxA was confirmed by cytotoxicity, Western blotting and SDS-PAGE and quantified with the Bio-Rad Protein Assay.

Confocal microscopy

Purified LtxA was labelled with FITC using a Pierce FITC antibody labelling kit (Thermo Fisher Scientific, Rockford, IL, USA) according to the manufacturer's instructions. Labelled LtxA (4 × 10⁻⁶ M) was added to 1 ml of Jurkat (Jn.9) cells (10⁶ cells ml⁻¹) and incubated at 37°C for 30 min. This toxin concentration was required to obtain a suitable fluorescence signal. The cells were then incubated for 10 min with WGA-AF594 (5 µg ml⁻¹) to stain the membranes. The cells were imaged at 100 × magnification on a Nikon A1 confocal microscope, equipped with an Ar laser and a 4-photomultiplier tube detector. The excitation wavelengths for FITC and WGA-AF594 were 488.0 and 561.4 nm, respectively and the emission wavelengths were 525.0 and 595.0 nm respectively.

SEM

LtxA (1 × 10⁻⁹ M) was added to 1 ml of Jurkat (Jn.9) cells (0.5 × 10⁶ ml⁻¹) and incubated at 37°C (Karakelian *et al.*, 1998; Fong *et al.*, 2006) for 30 min to 3 h. Aliquots were removed at various time points and immediately fixed in Karnofsky's fixative. The solutions were washed with ethanol and Freon and then

filtered. They were then mounted, coated with gold, and imaged on a JEOL 7500F high-resolution SEM (JEOL, Tokyo, Japan). Coronal slicing was performed with a FEI Strata DB235 FIB (FEI Company, Hillsboro, Oregon).

Calcein leakage

Liposomes to be used in the calcein leakage assay were prepared using the rapid solvent exchange technique (Buboltz and Feigenson, 1999). The required amounts of phospholipids, dissolved in chloroform were added to 7 ml glass scintillation vials. Warm calcein buffer (150 mM NaCl, 10 mM Tris, 1 mM EDTA, 100 mM calcein, pH = 7.4) was added, and the solution was vortex mixed while simultaneously exposed to vacuum (-20 bar). The resulting lipid solution was freeze-thawed five times, heated above the gel-liquid transition temperature (T_m), and extruded through a polycarbonate filter with 200 nm pores at least 11 times. Calcein-encapsulated liposomes were separated from free calcein by size exclusion chromatography in a column filled with Sephadex G-50, eluted with an isotonic column buffer (300 mM NaCl, 10 mM Tris, 1 mM EDTA, pH = 7.4).

Toxin-induced leakage was determined by measuring the release of calcein from liposomes. LtxA, rehydrated in the column buffer, was added to the calcein-encapsulating liposomes in the specified protein mole fractions and incubated at 30°C. Within the liposome, calcein was initially at a self-quenching concentration (100 mM); calcein release was measured by the increase in fluorescence intensity due to calcein dilution after toxin addition (I_F), relative to the baseline fluorescence intensity (I_B) and the fluorescence intensity after 100% leakage (I_T) obtained by adding 0.1% Triton X-100. The percentage of released calcein (%R) was determined by

$$\%R = (I_F - I_B) / (I_T - I_B) \quad (1)$$

The excitation wavelength was set at 490 nm, and the emission spectrum was recorded in the range of 500 to 550 nm, with excitation and emission slits set at 3 nm on a Perkin Elmer fluorescence spectrometer, model LS-55. A blank run in which buffer was added to the liposome suspension was subtracted from each sample run, so that the calculated release is due only to LtxA.

DSC

Measurements were made in a Nano II Differential Scanning Calorimeter (Calorimeter Sciences Corporation, Lindon, UT, USA). Lipid films of 1 mg of di16 : 1-PE were hydrated at room temperature with solutions of LtxA in 10 mM potassium phosphate at a pH of 6.5, to give the specified mole fractions of peptide. The mixtures were vortexed vigorously to make multilamellar vesicles and then degassed before loading into the sample cell of the calorimeter. Controls using peptide solutions in the sample cell in the absence of lipid showed no transition. Degassed buffer was placed in the reference cell. DSC was performed at a scan rate of 1.0 degree min⁻¹. Blank runs of buffer vs. buffer were subtracted from sample runs. Each point was collected using a fresh sample. The resulting curves were analysed by using the fitting program provided by Microcal (Northampton, MA, USA) and plotted with Origin version 7.0.

³¹P NMR

A lipid film was created by dissolving the required amounts of N-methyl-DOPE in chloroform in a glass vial. The chloroform was evaporated under a stream of nitrogen, and the residual chloroform was removed under vacuum. Multilamellar vesicles were created by hydrating the lipid film with buffer containing 150 mM NaCl and 10 mM HEPES at a pH of 7 to a final lipid concentration of 200 mM. Immediately before the NMR experiments, the concentrated liposome solution was mixed with an equal volume of either buffer or LtxA at a concentration of 20 μ M, creating a lipid : protein ratio of 10 000:1; the NMR samples also contained 10% D₂O.

The considerations for the acquisition of ³¹P NMR spectra of phospholipids have been reviewed by Yeagle and Kelsey (Yeagle and Kelsey, 1989). ³¹P spin echoes (Hahn, 1950) were acquired with the Meiboom-Gill modification (Meiboom and Gill, 1958) of the Carr-Purcell pulse sequence (Carr and Purcell, 1954). Specifically, a minimal two-echo scheme with a 5.2 μ s refocusing delay was used. All pulse receiver gating delays were set to zero. The pre-acquisition delay was adjusted in order to capture the echo peak and properly define the broad spectral components that correspond to the fastest decaying parts of the free induction decay (FID).

³¹P NMR spectra were acquired at the specified temperatures using a Varian INOVA NMR spectrometer (Agilent Technologies, Santa Clara, CA, USA), operating at a proton frequency of 499.9 MHz and equipped with a 5 mm dual broadband z-gradient probe. Typically, 2048 scans of 131 K complex data points over a 100 kHz spectral width were collected with a 1 s relaxation delay. All spectra were acquired with broadband proton decoupling gated on during acquisition and off during the remainder of the time.

The temperature-dependence study was conducted from low to high temperatures in order to avoid any possible kinetic barrier(s) to phase transition(s). As the temperature was raised, the sample changed from an off-white dispersion to a solution of white flocculants that floated outside the NMR probe coil region, resulting in the loss of NMR signal. This necessitated the use of water-matched Shigemi tubes, which restrict the whole sample within the coil region of the NMR probe.

Data sets were processed on a Sun Blade 100 workstation (Sun Microsystems, Palo Alto, CA, USA) using the VnmrJ software package (Agilent Technologies, Santa Clara, CA, USA). Exponential line broadening of 100 Hz was used throughout. The specifics of the NMR data acquisition removed the need for first-order phase corrections. The chemical shifts of the ³¹P NMR spectra are reported vs. the 85% H₃PO₄ chemical shift standard at 0.00 p.p.m.

Acknowledgements

The authors are grateful for technical expertise in SEM provided by Dr. Lolita Rotkina, Mr. Gerald Harrison and Dr. Douglas Yates.

References

- Allende, D., Simon, S.A., and McIntosh, T.J. (2005) Melittin-induced bilayer leakage depends on lipid material properties: evidence for toroidal pores. *Biophys J* **88**: 1828–1837.
- Alonso, A., Goni, F.M., and Buckley, J.T. (2000) Lipids favoring inverted phase enhance the ability of aerolysin to permeabilize liposome bilayers. *Biochemistry* **39**: 14019–14024.
- Anderluh, G., Serra, M.D., Viero, G., Guella, G., Macek, P., and Menestrina, G. (2003) Pore formation by Equinatoxin II, a eukaryotic protein toxin, occurs by induction of non-lamellar lipid structures. *J Biol Chem* **278**: 45216–45233.
- Bakas, L., Chanturiya, A., Herlax, V., and Zimmerberg, J. (2006) Paradoxical lipid dependence of pores formed by the *Escherichia coli* α -hemolysin in planar phospholipid bilayer membranes. *Biophys J* **91**: 3748–3755.
- Balakrishnan, L., Hughes, C., and Koronakis, V. (2001) Substrate-triggered recruitment of the TolC channel-tunnel during type I export of hemolysin by *Escherichia coli*. *J Mol Biol* **313**: 501–510.
- Balashova, N.V., Crosby, J.A., Al Ghofaily, L., and Kachlany, S.C. (2006) Leukotoxin confers beta-hemolytic activity to *Actinobacillus actinomycetemcomitans*. *Infect Immun* **74**: 2015–2021.
- Baumann, G., and Mueller, P. (1974) A molecular model of membrane excitability. *J Supramol Struct* **2**: 538–557.
- Benachir, T., and Lafleur, M. (1995) Study of vesicle leakage induced by melittin. *Biochim Biophys Acta* **1235**: 452–460.
- Benz, R., Schmid, A., Wagner, W., and Goebel, W. (1989) Pore formation by the *Escherichia coli* hemolysin: evidence for an association-dissociation equilibrium of the pore-forming aggregates. *Infect Immun* **57**: 887–895.
- Benz, R., Maier, E., Ladant, D., Ullmann, A., and Sebo, P. (1994) Adenylate cyclase toxin (CyaA) of *Bordetella pertussis*. evidence for the formation of small ion-permeable channels and comparison with HlyA of *Escherichia coli*. *J Biol Chem* **269**: 27231–27239.
- Benz, R., Hardie, K.R., and Hughes, C. (2005) Pore formation in artificial membranes by the secreted hemolysins of *Proteus vulgaris* and *Morganella morganii*. *Eur J Biochem* **220**: 339–347.
- Bhakdi, S., Mackman, N., Nicaud, J.M., and Holland, I.B. (1986) *Escherichia coli* hemolysin may damage target cell membranes by generating transmembrane pores. *Infect Immun* **52**: 63–69.
- Boesze-Battaglia, K., Fliesler, S.J., Li, J., Young, J.E., and Yeagle, P.L. (1992) Retinal and retinol promote membrane fusion. *Biochim Biophys Acta* **1111**: 256–262.
- Buboltz, J.T., and Feigenson, G.W. (1999) A novel strategy for the preparation of liposomes: rapid solvent exchange. *Biochim Biophys Acta* **1417**: 232–245.
- Burkhardt, J.K., Carrizosa, E., and Shaffer, M.H. (2008) The actin cytoskeleton in T cell activation. *Annu Rev Immunol* **26**: 233–259.
- Carr, H.Y., and Purcell, E.M. (1954) Effects of diffusion on free precession in nuclear magnetic resonance experiments. *Phys Rev* **94**: 630–638.
- Cheetham, J.J., Epand, R.M., Andrews, M., and Flanagan, T.D. (1990) Cholesterol sulfate inhibits the fusion of Sendai virus to biological and model membranes. *J Biol Chem* **265**: 12404–12409.
- Cherry, L.K., Weber, K.S.C., and Klickstein, L.B. (2001) A dominant Jurkat T cell mutation that inhibits LFA-1-mediated cell adhesion is associated with increased cell growth. *J Immunol* **167**: 6171–6179.

- Crosby, J.A., and Kachlany, S.C. (2007) TdeA, a TolC-like protein required for toxin and drug export in *Aggregatibacter (Actinobacillus) actinomycetemcomitans*. *Gene* **388**: 83–92.
- Cullis, P.R., and de Kruijff, B. (1979) Lipid polymorphism and the functional roles of lipids in biological membranes. *Biochim Biophys Acta* **559**: 299–420.
- Dileepan, T., Kachlany, S.C., Balashova, N.V., Patel, J., and Maheswaran, S.K. (2007) Human CD18 is the functional receptor for *Aggregatibacter actinomycetemcomitans* leukotoxin. *Infect Immun* **75**: 4851–4856.
- Ehrmann, I.E., Gray, M.C., Gordon, V.M., Gray, L.S., and Hewlett, E.L. (1991) Hemolytic activity of adenylate cyclase toxin from *Bordetella pertussis*. *FEBS Lett* **278**: 79–83.
- Ellens, H., Siegel, D.P., Alford, D., Yeagle, P.L., Boni, L., Lis, L.J., et al. (1989) Membrane fusion and inverted phases. *Biochemistry* **28**: 3692–3703.
- Epand, R.M. (2002) Diacylglycerols, lysolecithin, or hydrocarbons markedly alter the bilayer to hexagonal phase transition temperature of phosphatidylethanolamines. *Biochemistry* **24**: 7092–7095.
- Epand, R.M. (2007) Membrane lipid polymorphism. Relationship to bilayer properties and protein function. In *Methods in Membrane Lipids*. Dopic, A.M. (ed.). Totowa, NJ, USA: Humana Press, pp. 15–26.
- Fine, D.H., Furgang, D., Schreiner, H.C., Goncharoff, P., Charlesworth, J., Ghazwan, G., et al. (1999) Phenotypic variation in *Actinobacillus actinomycetemcomitans* during laboratory growth: implications for virulence. *Microbiology* **145**: 1335–1347.
- Fong, K.P., Pacheco, C.M.F., Otis, L.L., Baranwal, S., Kieba, I.R., Harrison, G., et al. (2006) *Actinobacillus actinomycetemcomitans* leukotoxin requires lipid microdomains for target cell cytotoxicity. *Cell Microbiol* **8**: 1753–1767.
- Fong, K.P., Tang, H.Y., Brown, A.C., Kieba, I.R., Speicher, D.W., Boesze-Battaglia, K., and Lally, E.T. (2011) *Aggregatibacter actinomycetemcomitans* leukotoxin is post-translationally modified by addition of either saturated or hydroxylated fatty acyl chains. *Mol Oral Microbiol* **26**: 262–278.
- Fuller, N., and Rand, R.P. (2001) The influence of lysolipids on the spontaneous curvature and bending elasticity of phospholipid membranes. *Biophys J* **81**: 243–254.
- van Gorkom, L.C.M., Nie, Q.S., and Epand, R.M. (1992) Hydrophobic lipid additives affect membrane stability and phase behavior of N-monomethyldioleoylphosphatidylethanolamine. *Biochemistry* **31**: 671–677.
- Gruner, S.M. (2005) Nonlamellar Lipid Phases. In *The Structure of Biological Membranes*. Yeagle, P.L. (ed.). Boca Raton, FL, USA: CRC Press, pp. 173–199.
- Hahn, E.L. (1950) Spin Echoes. *Phys Rev* **80**: 580–600.
- Iwase, M., Lally, E.T., Berthold, P., Korchak, H., and Taichman, N.S. (1990) Effects of cations and osmotic protectants on cytolytic activity of *Actinobacillus actinomycetemcomitans* leukotoxin. *Infect Immun* **58**: 1782–1788.
- Jarchau, T., Chakraborty, T., Garcia, F., and Goebel, W. (1994) Selection for transport competence of C-terminal polypeptides derived from *Escherichia coli* hemolysin: the shorted peptide capable of autonomous HlyB/HlyD-dependent secretion comprises the C-terminal 62 amino acids of HlyA. *Mol Gen Genet* **245**: 53–60.
- Kachlany, S.C., Fine, D.H., and Figurski, D.H. (2002) Purification of secreted leukotoxin (LtxA) from *Actinobacillus actinomycetemcomitans*. *Protein Expr Purif* **25**: 465–471.
- Karakelian, D., Lear, J.D., Lally, E.T., and Tanaka, J.C. (1998) Characterization of *Actinobacillus actinomycetemcomitans* leukotoxin pore formation in HL60 cells. *Biochim Biophys Acta* **1406**: 175–187.
- Kelk, P., Johansson, A., Claesson, R., Hanstrom, L., and Kalfas, S. (2003) Caspase 1 involvement in human monocyte lysis induced by *Actinobacillus actinomycetemcomitans* leukotoxin. *Infect Immun* **71**: 4448–4455.
- Kelk, P., Abd, H., Sandstrom, G., Sjostedt, A., and Johansson, A. (2011) Cellular and molecular response of human macrophages exposed to *Aggregatibacter actinomycetemcomitans* leukotoxin. *Cell Death and Dis* **2**: e126.
- Kieba, I.R., Fong, K.P., Tang, H.Y., Hoffman, K.E., Speicher, D.W., Klickstein, L.B., and Lally, E.T. (2007) *Aggregatibacter actinomycetemcomitans* leukotoxin requires β -sheets 1 and 2 of the human CD11a b-propeller for cytotoxicity. *Cell Microbiol* **9**: 2689–2699.
- Lally, E.T., Golub, E.E., Kieba, I.R., Taichman, N.S., Rosenbloom, J., Rosenbloom, J.C., et al. (1989) Analysis of the *Actinobacillus actinomycetemcomitans* leukotoxin gene. Delineation of unique features and comparison to homologous toxins. *J Biol Chem* **264**: 15451–15456.
- Lally, E.T., Kieba, I.R., Taichman, N.S., Rosenbloom, J., Gibson, C.W., Demuth, D.R., et al. (1991) *Actinobacillus actinomycetemcomitans* leukotoxin is a calcium-binding protein. *J Periodontal Res* **26**: 268–271.
- Lally, E.T., Golub, E.E., and Kieba, I.R. (1994) Identification and immunological characterization of the domain of *Actinobacillus actinomycetemcomitans* leukotoxin that determines its specificity for human target cells. *J Biol Chem* **269**: 31289–31295.
- Lally, E.T., Kieba, I.R., Sato, A., Green, C.L., Rosenbloom, J., Korostoff, J., et al. (1997) RTX toxins recognize a β 2 integrin on the surface of human target cells. *J Biol Chem* **272**: 30463–30469.
- Lally, E.T., Hill, B., Kieba, I.R., and Korostoff, J. (1999) The interaction between RTX toxins and target cells. *Trends Microbiol* **7**: 356–361.
- Lalonde, G., McDonald, T.V., Gardner, P., and O'Hanley, P.D. (1989) Identification of a haemolysin from *Actinobacillus pleuropneumoniae* and characterization of its channel properties in planar phospholipid bilayers. *J Biol Chem* **264**: 13559–13564.
- Lear, J.D., Furblur, U.G., Lally, E.T., and Tanaka, J.C. (1995) *Actinobacillus actinomycetemcomitans* leukotoxin forms large conductance, voltage-gated ion channels when incorporated into planar lipid bilayers. *Biochim Biophys Acta* **1238**: 34–41.
- Lee, M.-T., Hung, W.-C., Chen, F.-Y., and Huang, H.W. (2005) Many-body effect of antimicrobial peptides: on the correlation between lipid's spontaneous curvature and pore formation. *Biophys J* **89**: 4006–4016.
- Ludwig, A., Jarchau, T., Benz, R., and Goebel, W. (1998) The repeat domain of *Escherichia coli* haemolysin (HlyA) is responsible for is Ca^{2+} -dependent binding to erythrocytes. *Mol Gen Genet* **214**: 553–561.
- McCormick, J.I., and Johnstone, R.M. (1998) Volume enlargement and recovery of Na^{+} -dependent amino acid

- transport in proteoliposomes derived from Ehrlich ascites cell membranes. *J Biol Chem* **263**: 8111–8119.
- Maier, E., Reinhard, N., Benz, R., and Frey, J. (1996) Channel-forming activity and channel size of the RTX toxins ApxI, ApxII, and ApxIII of *Actinobacillus pleuropneumoniae*. *Infect Immun* **64**: 4415–4423.
- Martin, C., Requero, M.A., Masin, J., Konopasek, I., Goni, F.M., Sebo, P., and Ostolaza, H. (2004) Membrane restructuring by *Bordetella pertussis* adenylate cyclase toxin, a member of the RTX toxin family. *J Bacteriol* **186**: 3760–3765.
- Meiboom, S., and Gill, D. (1958) Modified spin-echo method for measuring nuclear relaxation times. *Rev Sci Instrum* **29**: 688–691.
- Menestrina, G., Mackman, N., Holland, I.B., and Bhakdi, S. (1987) *Escherichia coli* haemolysin forms voltage-dependent ion channels in lipid membranes. *Biochim Biophys Acta* **905**: 109–117.
- Moayeri, M., and Welch, R.A. (1997) Prelytic and lytic conformations of erythrocyte-associated *Escherichia coli* hemolysin. *Infect Immun* **65**: 2233–2239.
- Ortiz, A., Aranda, F.J., Villalain, J., San Martin, C., Micol, V., and Gomez-Fernandez, J.C. (1992) 1,2-Dioleoylglycerol promotes calcium-induced fusion in phospholipid vesicles. *Chem Phys Lipids* **62**: 215–224.
- Ortiz, A., Killian, J.A., Verkleij, A.J., and Wilschut, J. (1999) Membrane fusion and the lamellar-to-inverted-hexagonal phase transition in cardiolipin vesicle systems induced by divalent cations. *Biophys J* **77**: 2003–2014.
- Sansom, M.S. (1991) The biophysics of peptide models of ion channels. *Prog Biophys Mol Biol* **55**: 139–235.
- Siegel, D.P. (2005) Lipid membrane fusion. In *The Structure of Biological Membranes*. Yeagle, P.L. (ed.). Boca Raton, FL, USA: CRC Press, pp. 255–308.
- Siegel, D.P., and Tenchov, B.G. (2008) Influence of the lamellar phase unbinding energy on the relative stability of lamellar and inverted cubic phases. *Biophys J* **94**: 3987–3995.
- Tsai, C.-C., and Taichman, N.S. (1986) Dynamics of infection by leukotoxic strains of *actinobacillus actinomycetemcomitans* in juvenile periodontitis. *J Clin Periodontol* **13**: 330–331.
- Valcarcel, C.A., Serra, M.D., Potrich, C., Bernhart, I., Tejuca, M., Martinez, D., *et al.* (2001) Effects of lipid composition on membrane permeabilization by Sticholysin I and II, two cytolytic toxins of the sea anemone *Stichodactyla helianthus*. *Biophys J* **80**: 2761–2774.
- Yeagle, P.L., and Kelsey, D. (1989) Phosphorus nuclear magnetic resonance studies of lipid-protein interactions: human erythrocyte glycophorin and phospholipids. *Biochemistry* **28**: 2210–2215.
- Yeagle, P.L., and Sen, A. (1986) Hydration and the lamellar to hexagonal II phase transition of phosphatidylethanolamine. *Biochemistry* **25**: 7518–7522.
- Zambon, J.J. (1985) *Actinobacillus actinomycetemcomitans* in human periodontal disease. *J Clin Periodontol* **12**: 1–20.
- Zitzer, A., Bittman, R., Verbicky, C.A., Erukulla, R.K., Bhakdi, S., Weis, S., *et al.* (2001) Coupling of cholesterol and cone-shaped lipids in bilayers augments membrane permeabilization by the cholesterol-specific toxins Streptolysin O and *Vibrio cholerae* Cytolysin. *J Biol Chem* **276**: 14628–14633.